16th World Congress in Computational Mechanics (WCCM)
21-26 July 2024, Vancouver, Canada
A. Korobenko, M. Laforest, S. Prudhomme, R. Vaziri (Eds)

# DEVELOPMENT OF TRAFFIC NOISE EVALUATION SYSTEM USING FINITE ELEMENT METHOD

**HARUKI MIYAUCHI[1], KAZUO KASHIYAMA[2] AND HITOSHI YOSHIKAWA[3]**

[1] Graduate School of Civil, Human and Environmental Engineering, Chuo University
Kasuga 1-13-27, Bunkyo-ku, Tokyo 112-8551, JAPAN
a19.65sn@g.chuo-u.ac.jp

[2] Department of Civil and Environmental Engineering, Chuo University
Kasuga 1-13-27, Bunkyo-ku, Tokyo 112-8551, JAPAN
kaz@civil.chuo-u.ac.jp

[3] Graduate School of Advanced Integrated Studies in Human Survivability
Yoshidanakaadachi-cho 1, Sakyo-ku, Kyoto 606-8306, JAPAN
yoshikawa.hitoshi.5u@kyoto-u.ac.jp

**Key words:** Finite Element Method, Noise Barrier, Virtual Reality, Auralization.

**Abstract.** This paper presents a traffic noise evaluation system based on acoustic theory. The finite element method is employed for unsteady wave equations, which is suitable for arbitrary shapes and has excellent applicability to non-uniform materials. The 3D wave equation is employed for the governing equation and the Perfectly Matched Layer (PML) method is utilized as a treatment method for boundary condition. In order to consider multiple moving sound sources such as a traffic noise, a time-variant convolution method is introduced. The auralization method based on VR technology is also introduced to understand the noise level intuitively.

## 1 INTRODUCTION

Noise is one of the seven major types of pollution in Japan, and it leads to the highest number of complaints according to a survey published by the Ministry of Internal Affairs and Communications in December 2023. Especially in urban areas, the evaluation of noise has been an urgent issue in the planning and designing of various constructions, such as roads, railways, and airports. In recent years, numerical simulation has been widely used based on geometric sound theory and wave sound theory as a noise evaluation method.

We have developed a sound field analysis method using the time-domain fast multipole boundary element method based on wave sound theory [1]. However, the boundary element method has a problem in that the material of the computational model is not considered strictly. Therefore, we aim to consider the propagation of sound in the internal structure of the noise barrier by using the finite element method [2].

In this study, we present the development of a sound field analysis method using the finite element method based on the impulse response analysis method. The 3D wave equation is employed for the governing equation and the Perfectly Matched Layer (PML) method [3]-[5] is utilized as a treatment method for boundary condition. In order to consider multiple moving sound sources such as a traffic noise, a time-variant convolution method [6] is introduced. In addition, the auralization method based on VR technology is also introduced to understand the noise level intuitively.

## 2 NUMERICAL ANALYSIS METHOD

### 2.1 Governing equation and conditional expression

For the governing equations, the 3D unsteady modified wave equation is employed to use the PML method and advection equations to obtain auxiliary variables.

$$\frac{\partial^2 p}{\partial t^2} + \alpha \frac{\partial p}{\partial t} + \beta p - c^2 \frac{\partial^2 p}{\partial x_j \partial x_j} - c^2 \frac{\partial \Phi_j}{\partial x_j} = 0 \quad \text{in } D, \tag{1}$$

$$\frac{\partial \Phi_i}{\partial t} + \mathbf{A}\Phi_i + \mathbf{B}\frac{\partial p}{\partial x_i} = 0 \quad \text{in } D_{\text{pml}}, \tag{2}$$

where $D$ is the computational domain, $D_{\text{pml}}$ is the PML domain, $x_i, x_j$ are the coordinates in 3D space, $t$ is time, $c$ is sound velocity, $p$ is sound pressure, and $\Phi_i$ are auxiliary variables for applying PML. The following shows each variable and its matrix.

$$\alpha = \sigma_x + \sigma_y + \sigma_z, \tag{3}$$

$$\beta = \sigma_x\sigma_y + \sigma_y\sigma_z + \sigma_z\sigma_x, \tag{4}$$

$$\mathbf{A} = \begin{bmatrix} \sigma_x & 0 & 0 \\ 0 & \sigma_y & 0 \\ 0 & 0 & \sigma_z \end{bmatrix}, \tag{5}$$

$$\mathbf{B} = \begin{bmatrix} \sigma_x - \sigma_y - \sigma_z & 0 & 0 \\ 0 & \sigma_y - \sigma_z - \sigma_x & 0 \\ 0 & 0 & \sigma_z - \sigma_x - \sigma_y \end{bmatrix}, \tag{6}$$

where $\sigma_x, \sigma_y, \sigma_z$ represent the attenuation parameters in each direction, which are non-zero in PML domain and zero in the computational domain, and absorb sound waves. In addition, $\sigma_x, \sigma_y, \sigma_z$ are obtained by the following equation.

$$\sigma_{x_i}(d_i) = \begin{cases} 0 & |d_i| < a_i, \\ -\dfrac{3c\ln R}{2L_i}\left(\dfrac{d_i - a_i}{L_i}\right)^2 & a_i \le |d_i| \le a_i + L_i, \end{cases} \tag{7}$$

where $L_i$ is the thickness of the PML in each direction,,$a_i$ is the boundary coordinate value between the PML and computational domain, $d_i$ is an arbitrary position coordinate, and $R$ is the theoretical coefficient of reflection. Since $\sigma_x, \sigma_y, \sigma_z$ and $\Phi_i$ are zero in the computational domain, it is equivalent to solving the ordinary wave equation.

### 2.2 Initial and Boundary Conditions

The following silence conditions are assumed as initial conditions.

$$p = 0 \quad \text{in} \quad D, \tag{8}$$

$$\frac{\partial p}{\partial t} = 0 \quad \text{in} \quad D, \tag{9}$$

The following boundary conditions are employed.
Dirichlet boundary condition：

$$p = \hat{p} \quad \text{on} \quad \partial D_p, \tag{10}$$

Neumann boundary condition：

$$\frac{\partial p}{\partial n} = 0 \quad \text{on} \quad \partial D_q, \tag{11}$$

where $\partial D_p, \partial D_q$ are the Dirichlet and Neumann boundary conditions, $\hat{p}$ is the known sound pressure, and $n$ is the outward unit normal vector. Equation (11) is the boundary condition for perfect reflection.

### 2.3 Finite Element Method

The weighted residual method based on Galerkin method is employed for equation(1), (2). The following weak forms are obtained.

$$\int_D p^* \frac{\partial^2 p}{\partial t^2} d\Omega + \alpha \int_D p^* \frac{\partial p}{\partial t} d\Omega + \beta \int_D p^* p d\Omega + c^2 \int_D \frac{\partial p^*}{\partial x_j} \frac{\partial p}{\partial x_j} d\Omega - c^2 \int_D p^* \frac{\partial \Phi_j}{\partial x_j} d\Omega = c^2 \int_{\partial D_q} p^* \frac{\partial p}{\partial n} d\Gamma, \tag{12}$$

$$\int_D \Phi_i^* \frac{\partial \Phi_i}{\partial t} d\Omega + \mathbf{A} \int_D \Phi_i^* \Phi_i d\Omega + \mathbf{B} \int_D \Phi_i^* \frac{\partial p}{\partial x_i} d\Omega = 0, \tag{13}$$

where $p^*, \Phi^*$ is the weight function of $p, \Phi$. The subscript "$e$" indicates that the calculation is for each element. We use tetrahedral first-order elements for the spatial discretization for equation (12), (13) to derive the following finite element equation.

$$\mathbf{M}_e \frac{\partial^2 \mathbf{p}}{\partial t^2} + \alpha \mathbf{M}_e \frac{\partial \mathbf{p}}{\partial t} + \beta \mathbf{M}_e \mathbf{p} + \mathbf{K}_e \mathbf{p} - \mathbf{S}_e \mathbf{\Phi}_j = \mathbf{F}_e, \tag{14}$$

$$\mathbf{M}_e \frac{\partial \mathbf{\Phi}_i}{\partial t} + \mathbf{A} \mathbf{M}_e \mathbf{\Phi}_i + \mathbf{B} \mathbf{S}_e \mathbf{p} = 0, \tag{15}$$

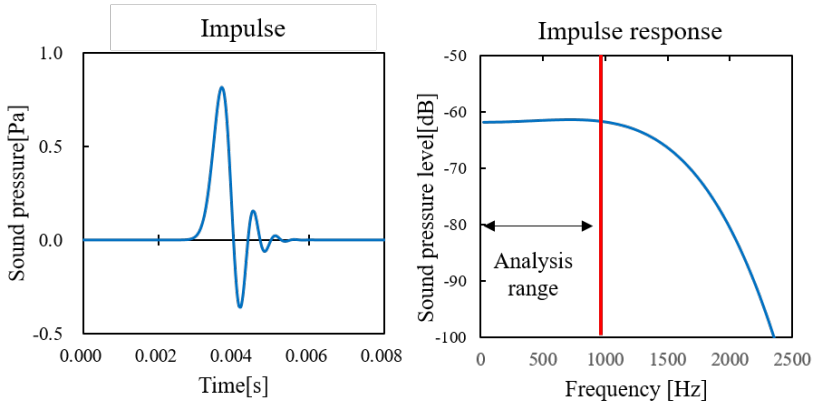


**Figure 1**: Pseudo impulse of Lubich

where $\mathbf{M}_e$ is the mass matrix, $\mathbf{K}_e$ is the diffusion matrix, $\mathbf{S}_e$ is the advection matrix and $\mathbf{F}_e$ is the boundary integral term. Then, superimposing equations (14) and (15) for all elements, we obtain the finite element equations for the entire system. Using the difference method for discretization in the time direction and lumping the mass matrix to apply the explicit method, the following discretization equations are obtained.

$$\bar{\mathbf{M}}\mathbf{p}^{n+1} = \bar{\mathbf{M}}(2\mathbf{p}^n - \mathbf{p}^{n-1}) + (\sigma_x+\sigma_y+\sigma_z)\bar{\mathbf{M}}(\mathbf{p}^n - \mathbf{p}^{n-1}\Delta t) + (\sigma_x\sigma_y+\sigma_y\sigma_z+\sigma_z\sigma_x)\bar{\mathbf{M}}\mathbf{p}^n\Delta t^2 - \mathbf{K}\mathbf{p}^n\Delta t^2 + \mathbf{S_x}\mathbf{\Phi}_x^n\Delta t^2 - \mathbf{S_y}\mathbf{\Phi}_y^n\Delta t^2 - \mathbf{S_z}\mathbf{\Phi}_z^n\Delta t^2 + \mathbf{F}\Delta t^2, \quad (16)$$

$$\bar{\mathbf{M}}\mathbf{\Phi}_x^{n+1} = (1-\sigma_x\Delta t)\bar{\mathbf{M}}\mathbf{\Phi}_x^n - (\sigma_x - \sigma_y - \sigma_z)\mathbf{S_x}\mathbf{p}^n\Delta t, \quad (17)$$

$$\bar{\mathbf{M}}\mathbf{\Phi}_y^{n+1} = (1-\sigma_y\Delta t)\bar{\mathbf{M}}\mathbf{\Phi}_y^n - (\sigma_y - \sigma_z - \sigma_x)\mathbf{S_y}\mathbf{p}^n\Delta t, \quad (18)$$

$$\bar{\mathbf{M}}\mathbf{\Phi}_z^{n+1} = (1-\sigma_z\Delta t)\bar{\mathbf{M}}\mathbf{\Phi}_z^n - (\sigma_z - \sigma_x - \sigma_y)\mathbf{S_z}\mathbf{p}^n\Delta t, \quad (19)$$

where $\bar{\mathbf{M}}$ is the lumped mass matrix.

### 2.4 Impulse Response Analysis

We create auralization sound by using impulse response analysis method, compare the effectiveness of sound insulation, and develop a noise evaluation system. In this study, the weights $\omega_n(\Delta t)$ of the discretized convolution integral in the method for obtaining the convolution integral by discrete approximation proposed in Lubich's CQM (Convolution Quadrature Method)[7], an approximate solution method for the convolution integral, are used as input waves.

$$\omega_n(\Delta t) = \frac{R^{-n}}{L}\sum_{l=0}^{L-1}\left(\frac{1}{4\pi r}e^{-\frac{s}{c}r}\right)e^{(-2\pi i\frac{nl}{L})}, \quad (20)$$

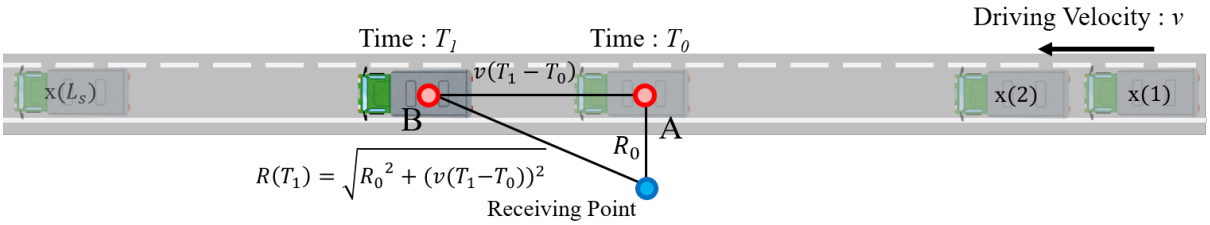


**Figure 2**: Estimation method for moving sound sources

where $r$ is the distance from the source, $n$ is the time step, $L$ is the number of divisions in the integration interval, $R$ is expressed as $R = \epsilon^{1/2L}$ and $s$ as $s = \gamma(\zeta)/\Delta t$ using the target accuracy $\epsilon$. The $\gamma(\zeta)$ is the quotient of the generating polynomial in the linear multi-step method (difference method). **Figure 1** shows the time history and frequency response of the pseudo-impulse response generated by the (20). This impulse has a feature that has a constant frequency until a certain section and decays sharply at higher frequencies. This feature means that it prevents from occurring analysis errors by high frequency. Here, $r$ and $\Delta t$ are assumed to be $r$ = 1.2m, and $\Delta t$ = 0.0667ms respectively, the analysis range is until 1000Hz.

### 2.5 Time-Variant Convolution Method

Let $x(t)$ denote each position of the moving sound source, $h(t, x(t))$ denote the impulse response from the fixed source to the sound receiving point at position $x(t)$, and $s(t)$ denote the source signal. The sound pressure $p(t)$ at the sound receiving point at each position at each time is given by the wave equation for a moving sound source and can be expressed approximately as (21).

$$p(k) = \sum_{k_s=0}^{\infty} s(k_s) h(k - k_s, x(k_s)), \tag{21}$$

In addition, the expression (21) can be expressed in the form of a matrix operation as follows[6].

$$\mathbf{p} = \mathbf{H}\mathbf{s}, \tag{22}$$

$$\mathbf{H} = \begin{bmatrix} h(1,\mathbf{x}(1)) & 0 & \cdots & 0 \\ h(2,\mathbf{x}(1)) & h(1,\mathbf{x}(2)) & \ddots & \vdots \\ \vdots & h(2,\mathbf{x}(2)) & \ddots & 0 \\ h(L_h,\mathbf{x}(1)) & \vdots & \ddots & h(1,\mathbf{x}(L_s)) \\ 0 & h(L_h,\mathbf{x}(2)) & \ddots & h(2,\mathbf{x}(L_s)) \\ \vdots & \ddots & \ddots & \vdots \\ 0 & \cdots & 0 & h(L_h,\mathbf{x}(L_s)) \end{bmatrix}, \tag{23}$$

where $\mathbf{s}$ is the source signal vector, $\mathbf{p}$ is the received signal vector, $\mathbf{H}$ is the time-varying convolution matrix, $L_s$ is the source signal length, and $L_h$ is the impulse response length. In creating

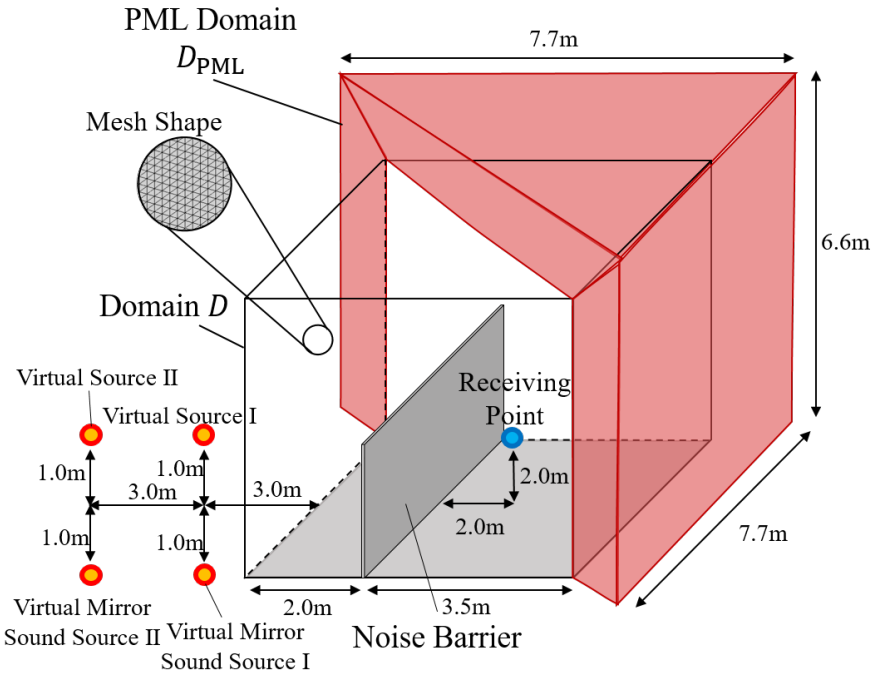


**Figure 3**: Numerical model

the time-variant convolution matrix, it is necessary to obtain the impulse responses from all the source locations, but there is a limit to the impulse responses that can be obtained. Therefore, the impulse response at each position is obtained by distance decay from the reference point using the method shown in **Figure 2**. In **Figure 2**, $v$ is the assumed velocity of the source, $T_0$ is the reference time, $T_1$ is any time, and $R_0$ is the distance between the source and the receiver point at the reference time.

## 3 EXAMPLE OF NUMERICAL ANALYSIS

### 3.1 Numerical Condition

The numerical model is shown in **Figure 3**. The sound velocity, time increment width, and spatial discretization width are set to $340\mathrm{m/s}$, $6.67 \times 10^{-5}\mathrm{s}$, and $0.022\mathrm{m}$, respectively, and pseudo impulse of Lubich is used as the input wave. The PML parameters are $L_i = 1.1\mathrm{m}$ and $R = 10^{-6}$. The number of degrees of freedom is approximately 80 million. Regarding the sound source location, virtual sound source T is placed at a distance of 3.0 m orthogonally from the center of the noise barrier, and virtual sound source Ⅱ is placed at a distance of 6.0 m orthogonally from the center of the noise barrier. Virtual sound source I is the position of the vehicle traveling on the side of the noise barrier, and virtual sound source Ⅱ is the position of the sound source of the oncoming vehicle. The sound source for auralization was a stationary version of the driving noise of large vehicles, medium-sized vehicles, and motorcycles.

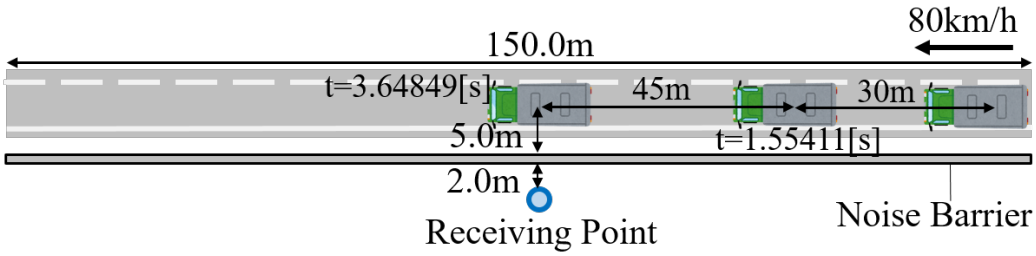


**Figure 4**: Driving condition for visualization

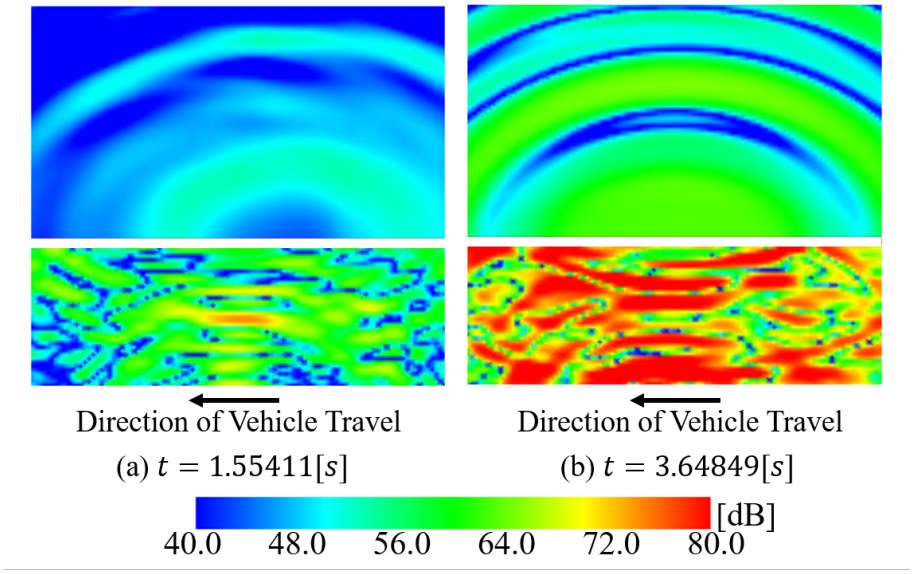


**Figure 5**: Time-variant convolution operation results for orthogonal horizontal section of noise barrier

### 3.2 Numerical Result

A time-variant convolution operation is performed on the impulse response obtained at the sound receiving point to make it audible. Driving conditions for visualization are shown in **Figure 4**. It is assumed that a $150\mathrm{m}$ section is driven at a speed of $80\mathrm{km/h}$. A visualization of the results of the time-variant convolution calculation with the noise source of a large vehicle in the horizontal cross section orthogonal to the noise barrier is shown in **Figure 5**. We found reduction in sound pressure level behind the noise barrier and movement of the sound source. Driving conditions for visualization are shown in **Figure 6**. It is assumed that medium-sized vehicles, large vehicles, and motorcycles drive at a speed of 80 km/h with a distance of 80 m between vehicles, in that order, on a 150 m section. **Figure 7** shows the time history waveforms at the sound receiving point when each lane runs simultaneously and when only the lane on the side of the noise barrier. We found that the sound source represents the characteristics

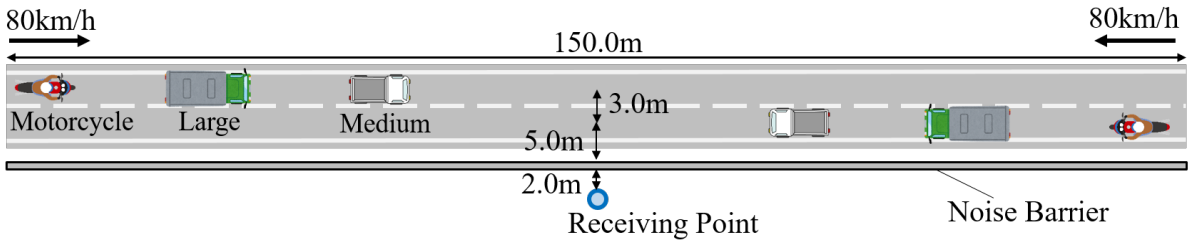


**Figure 6**: Driving condition for auralization

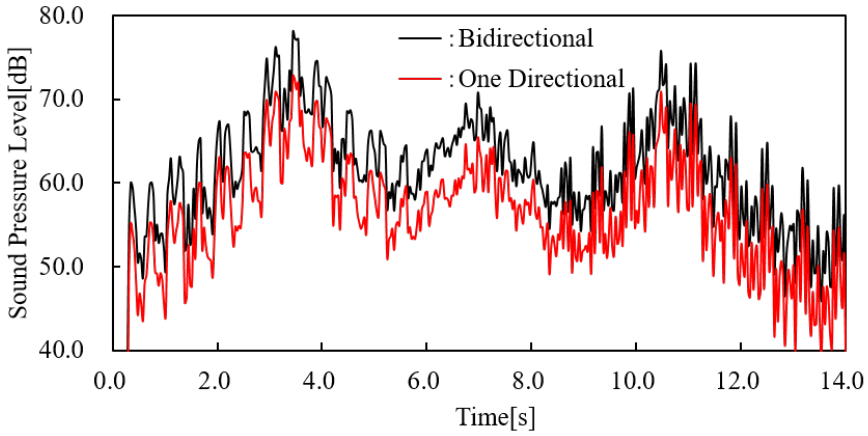


**Figure 7**: Time history waveforms

of a moving sound source, which gradually becomes louder as the source approaches from a distance and becomes quieter as it moves away, and that the sound pressure level also becomes louder due to bidirectional driving.

## 4 VIRTUAL REALITY SYSTEM BASED ON HMD

Time-variant convolution operations were performed at the sound receiving point, and the results obtained are used to develop a visualization and auralization system using VR technology. The device used is MetaQuest3 **Figure 9** shown in . The system follows the flowchart shown in **Figure 8**. The data obtained by numerical analysis of the convolution result with the real sound source at the sound receiving point is read, and the visualization side uses Unity to draw the surrounding environment by CG and create a stereoscopic image, and the auralization side uses the 3D Sound Settings function in Unity's Audio Source to create a stereoscopic sound. These results are presented by the device's screen and speakers. The vehicle to be driven is determined using random numbers, and after the vehicle to be driven is determined, the calculation results are superimposed in the system to reproduce random driving that is close to the actual phenomenon. The system experience is shown in **Figure 10**.

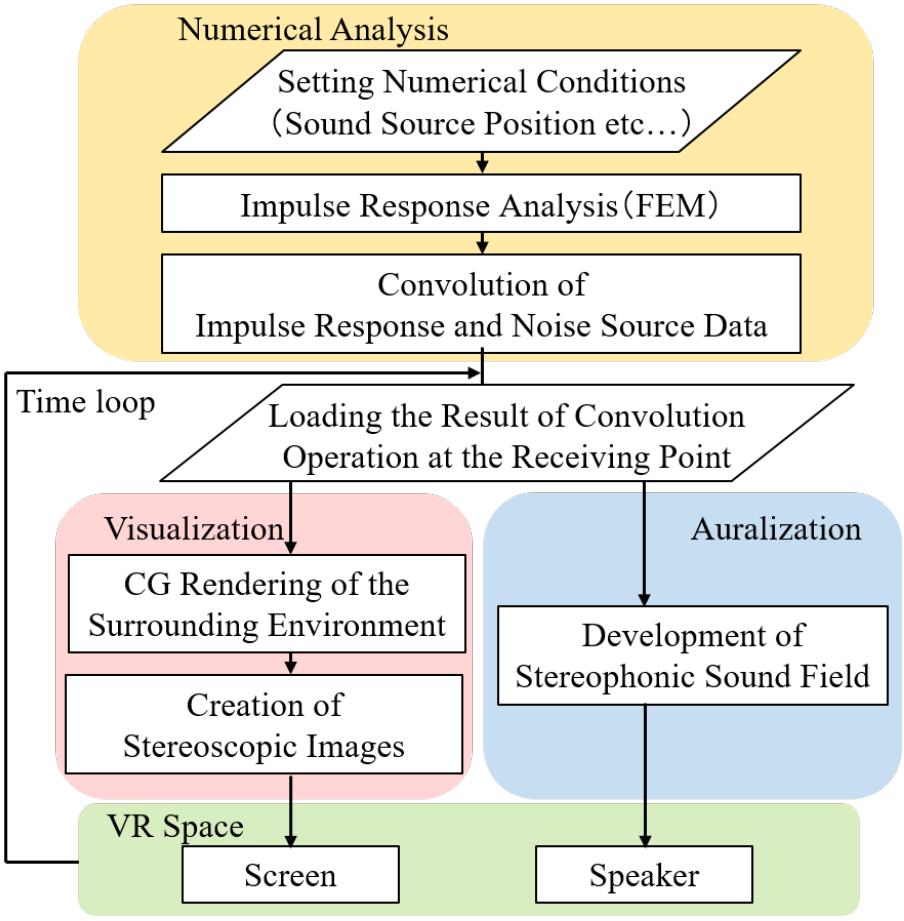


**Figure 8**: Flowchart

## 5 CONCLUSIONS

In this study, a traffic noise evaluation system based on the finite element method using PML has been developed. In order to show the validity of the system, the system has been applied to the traffic noise problem with multiple vehicles, and the following conclusions are obtained.

- We have confirmed that the system can reproduce the traffic noise by superimposing time-variant convolutional operations.
- The present noise evaluation system based on HMD is useful for planning and designing tools, and also for consensus building for the local residents.

We plan to consider the internal structure of noise barriers for future work.

**Figure 9**: Meta Quest 3


**Figure 10**: VR system

## REFERENCES

[1] Takahashi, T. An interpolation-based fast-multipole accelerated boundary integral equation method for the three-dimensional wave equation. *Journal of Computational Physics.* (2014) **258**:1-12.

[2] Nomura, T., Takagi, k. and Sato, S. Finite element simulation of sound propagabion concerning meteorological conditions. *International Journal for Numerical Methods in Fluids.* (2010) **64**:1296-1318.

[3] Berenger, K. A perfectly matched layer for the absorption of electromagnetic waves. *Journal of Computational Physics.* (1994) **114**:185-200.

[4] Kaltenbacher, B. Kaltenbacher, M. and Sim, I. A modified and stable version of a perfectly matched layer technique for the 3-d second order wave equation in time domain with an application to aeroacoustics. *Journal of Computational Physics.* (2013) **235**:407-422.

[5] Zhou, F. Ma, Q. and Gao, B. Efficient unsplit perfectly matched layers for finite-element time-domain modeling of elastodynamics. *Journal of Engineering Mechanics.* (2016) **142**:1-12.

[6] Matsumoto, M. Tohyama, M. and Yanagawa, H. A method of interpolating binaural impulse responses for moving sound images. *Acoustical Science and Technology* (2003) **24**:284-292.

[7] Lubich, C. Convolution quadrature and discretized operational calculus. I. *Numerische Mathematik.* (1988) **52**:129-145.